Optical chemosensors for metal ions in aqueous medium with polyfluorene derivatives: Sensitivity, selectivity and regeneration

Xinyang Wang, Qiqiao Lin, Sasikumar Ramachandran, Gaëlle Pembouong, Robert Bernard Pansu, Isabelle Leray, Bérengère Lebental, Gaël Zucchi

Optical chemosensors for metal ions in aqueous medium with polyfluorene derivatives: sensitivity, selectivity and regeneration

Xinyang Wang,[a] Qiqiao Lin,[a] Sasikumar Ramachandran,[a] Gaëlle Pembouong,[b] Robert B. Pansu,[c] Isabelle Leray,[c] Bérengère Lebental, [a,d] Gaël Zucchi*[a]

[a] LPICM, CNRS, Ecole polytechnique, Université Paris-Saclay, 91128, Palaiseau, France. Email : gael.zucchi@polytechnique.edu.

[b] Sorbonne Universités, UPMC Univ Paris 06, CNRS, IPCM, Chimie des Polymères, 75005 Paris, France.

[c] Laboratoire PPSM ENS Paris-Saclay CNRS, UMR 8531, Institut d'Alembert IFR 121, 61, avenue du Président Wilson, 94235Cachan Cedex, France.

[d] Université Paris-Est, IFSTTAR, COSYS, Marne-la-Vallée 77447, France.

Abstract

Six polyfluorene derivatives, **P1**–**P6**, were synthesized and investigated as responsive materials for the optical sensing of metal ions in an aqueous medium. They were designed by combining carbazole with fluorene units within the backbone. Carbazole was *N*-functionalized with three coordinating groups, 2-pyridyl-benzimidazole (**P1** and **P4**), 2-phenyl-benzimidazole (**P2** and **P5**) and 4-phenyl-terpyridyl (**P3** and **P6**), respectively. **P1**–**P3** are random copolymers with fluorene:carbazole ratios of 9:1 for **P1** and **P2**, and 9.7:0.3 for **P3**; **P4**–**P6** are the corresponding alternating polymers. This design lead to polymers made of a conjugated backbone and pendant

coordinating groups. The optical properties of the monomers were impacted in various ways by metal ions, and the formation of the [Ni**M3**]$^{2+}$ and [Zn**M3**]$^{2+}$ and [Zn**M3**$_2$]$^{2+}$ were evidenced with association constants of $10^{5.22}$, $10^{6.45}$ and $10^{14.0}$, respectively. The emission of the polymers was afterwards found to be influenced by theses metal ions with different sensitivity and selectivity. **P1** was found to be more sensitive to the Ni^{2+} and Cu^{2+} ions with a better selectivity for Ni^{2+}. Emission of the corresponding alternating polymer **P4** was more efficiently quenched by these two ions with respect to **P1**, in addition of being sensitive to the Ca^{2+} and Al^{3+} ions. **P3** showed sensitivity to the Ni^{2+}, Cu^{2+}, Al^{3+}, Ca^{2+}, and Zn^{2+} ions. The luminescence of **P6** was much more pronounced with the Ni^{2+}, Cu^{2+}, Cd^{2+}, Zn^{2+}, Al^{3+}, Fe^{2+}, and Fe^{3+} ions with respect to **P3**. More remarkably, the presence of the Zn^{2+} or Cd^{2+} ions resulted in a new emission band, leading to the possibility to selectively sense these two ions. Relatively high Stern-Volmer constants (in the 10^6–10^5 range) were obtained, and sensitivities down to the ppb level were reached, especially for the Ni^{2+} ion. Influence of both the coordinating group and the polymer backbone on the polymers sensitivity and selectivity was emphasized. Finally, the recyclability of some representative optical sensors was shown both in solution and in the solid state. In particular, thin films were shown to be easily regenerated, which opens the way to the elaboration of reusable optical sensors.

Keywords

Optical sensors, conjugated polymers, luminescence spectroscopy, metal ions.

1. Introduction

Analysis of water contaminants that are toxic for human being and aquatic life is of primary importance. Especially, the measurements of the quality of drinking water delivered in private dwellings is a significant public health concern. Metals represent a family of undesired contaminants. The elevated concentration of metal ions in water is mostly due to human activity

(industry, farming, and housing). These ions may cause various organ damages and are notably linked to widespread brain diseases such as Parkinson's and Alzheimer's diseases. [1-5] Respiratory and cardiac problems can be caused by nickel ingestion, [6] and accumulation of the Ni^{2+} ion in the body leads to oxidative stress. [7] Ni^{2+} and Cu^{2+} are also noxious to teeth and bones. These negative effects result from the formation of coordination complexes between the metal ions and biological matter.

Most of the metals are toxic at the ppb level (μg/L). The World Health Organization (WHO) set the provisional maximum tolerable daily intake to 2 ppm (mg/L) for Cu^{2+}, 200 ppm for Ca^{2+}, and 70 and 10 ppb for Ni^{2+} and Pb^{2+}, respectively, for drinking water. It is thus of primary importance to be able to accurately determine their concentration in water at such low levels.

Optical spectroscopy is a technique widely used for metal detection as low detection limits with high sensitivities can be reached when highly emissive probes are used. Polyfluorene derivatives are a class of polymers known to show high quantum yields both in solution and deposited as thin films. [8] They feature a strong synergy between semiconducting and emissive properties and were primarily developed as sensing materials for the optical detection of explosives in the second half of the nineties by Swager and co-workers. [9] They showed that the exciton transport properties of semiconducting fluorescent organic polymers enabled a large amplification of the signal for detection of nitroaromatic explosive materials. Since then, studies dealing with the measurement of species in solution, both in organic and aqueous media, have been reported. Both chemical and biological substances are targeted in this approach, among which inorganic cations, in particular metal ions, [10-13] inorganic anions such as halides, [14,15] or organic compounds such as aromatic amines. [16] Note that only a few of these described solid state sensors.

We describe herein the synthesis of polyfluorene derivatives functionalized with pendant coordinating groups and their use to design both solution and solid-state optical sensors for probing the presence of physiologically or environmentally important metal ions in an aqueous environment. The possibility to regenerate these sensors is discussed.

2. Experimental

2.1. Materials and instruments

3,6-dibromocarbazole, 2-(2-Pyridyl)benzimidazole, 2-Phenylbenzimidazole, phenylboronic acid pinacol ester, bromobenzene, 2-acetylpyridine, tetraethylammonium hydroxide (20% in H_2O), tri(*p*-tolyl)phosphine and palladium(II) acetate, and the metal salts were purchased from VWR and used as received, as well as ethanol and 1,4-dioxane. 9,9-di-*n*-octylfluorene-2,7-diboronic acid bis(pinacol) ester was purchased from Alfa Aesar, and 9,9-dihexyl-2,7-dibromofluorene was purchased from Aldrich. 3,6-dibromo-9-hexyl-9H-carbazole, [17] 3,6-Dibromo-9-(*N*-(2-(2'-pyridyl)-benzimidazole)-hexyl)-carbazole (**M1**), [18] and 9-(6-(2-Phenyl-*1H*-benzo[d]imidazol-1-yl)hexyl)-9H-carbazole (**M2**), [19] 4-(9H-carbazol-9-yl)benzaldehyde [20] and 4-(3,6-dibromo-9H-carbazol-9-yl)benzaldehyde [21] were synthesized from reported procedures as well as Poly(9,9-di-*n*-hexyl-2,7-fluorene) (**PF**). [8] Toluene, DMF and the aqueous solution of tetraethylammonium hydroxide (TEAH) were degassed prior to use. All reactions were performed under an inert atmosphere of argon.

NMR spectra have been recorded on a Bruker Avance 300 spectrometer; chemical shifts are given with respect to TMS (δ= 0). GPC measurements were done with Viscotek equipment using THF as solvent and polystyrene as standard. The UV-Vis absorption spectra were recorded using a JENWAY UV-VIS Spectrophotometer Model UV 6800. THF was used as solvent. The photoluminescence spectra were recorded using a HORIBA Jobin Yvon Spectrofluorometer Model Fluoromax-4.

2.2. Synthesis

9-(4-([2,2':6',2''-terpyridin]-4'-yl)phenyl)-3,6-dibromo-9H-carbazole (**M3**). 4-(3,6-dibromo-9H-carbazol-9-yl)benzaldehyde (1.2 mmol, 500 mg) was dissolved in a mixture of 14 ml of ethanol and 30 ml of 1,4-dioxane in a round bottom flask. 2-Acetylpyridine (2.4 mmol, 324 µl), KOH (3.6 mmol, 200 mg) and 10 ml NH_3 aq. (29%) were added successively to the flask. The mixture was stirred at 75°C overnight. Afterwards the solvents were evaporated *in vacuo*. The residue was dissolved in chloroform, extracted with water and a saturated sodium chloride solution. The organic phase was washed with water. After drying over magnesium sulfate, the organic extracts were evaporated and the crude product was purified by precipitation in chloroform and hexane. **M3** was obtained as a white powder (295 mg, 40%).

^{1}H NMR (300 MHz, $CDCl_3$) δ 8.83 (d, 2H, $H_{terpyridine}$), 8.78-8.67 (m, 4H, $H_{terpyridine}$), 8.22 (d, J = 1.9 Hz, 2H), 8.17-8.12 (m, 2H, $H_{carbazole}$), 7.91 (td, J = 7.7Hz, 1.8Hz, 2H), 7.69-7.63 (m, 2H), 7.55 (dd, J = 8.7Hz, 1.9 Hz, 2H, $H_{carbazole}$), 7.39 (ddd, J = 7.5Hz, 4.8Hz, 1.2 Hz, 2H, $H_{terpyridine}$), 7.33 (d, J = 8.7Hz, 2H, $H_{carbazole}$) ; ^{13}C NMR (75 MHz, $CDCl_3$, ppm) δ 156.05, 156.00, 149.13, 149.03, 137.36, 136.94, 132.09, 128.88, 123.96, 121.39, 118.54. HRMS (ESI, m/z): calcd. for $C_{33}H_{20}Br_2N_4^+$ 630.01, found 630.0.

.

General procedure for polymers synthesis. The polymers were obtained from Suzuki-Myiaura coupling following the procedure previously reported. [8]

Poly(9,9-dihexylfluorene-co-(pyridine-benzimidazole) carbazole) (**P1**).

Yield: 56 %; ^{1}H NMR (400 MHz, $CDCl_3$, ppm) δ 8.67 (m, 2H, ArH), 8.42 (m, 3H, ArH), 8.06 (m, 1H, ArH), 7.92 (m, 1H, ArH), 7.78 (m, 10H, ArH), 7.63 (m, 19 H, ArH), 7.42 (m, 7H, ArH), 4.84(m, 2H, Cz-H), 4.33 (m, 2H, Cz-H), 2.08 (br, 24H), 1.44(br, 14H), 1.06 (m, 60H), 0.71(br, 48H, CH_3) ; ^{13}C NMR (101 MHz, $CDCl_3$) δ 150.77, 150.65, 148.73, 147.58, 139.49, 139.30, 139.19, 138.98, 135.77, 135.45, 127.75, 127.53, 126.16, 125.12, 123.68, 122.72,

122.57, 122.30, 121.60, 120.48, 118.95, 109.12, 54.30, 44.23, 39.35, 30.46, 30.44, 28.65, 25.91, 25.64, 25.53, 22.82, 21.56, 21.54, 13.05, 13.01, 12.99 ; M_n = 10.8 kDa; M_w = 30.5 kDa.

The average amount of the carbazole unit in the polymer chain is calculated to be 11% according to the ^{1}H NMR spectrum by comparing the intensity of the signal at 4.84 ppm and 4.33 ppm attributed to Cz-H of **M1** with the intensity of the signal at 0.71 ppm attributed to the CH_3 groups of the fluorene hexyl chains.

Poly(9,9-dihexylfluorene-co-(phenyl-benzo-imidazole) carbazole) (**P2**).

Yield: 45%; ^{1}H NMR (300 MHz, $CDCl_3$, ppm) δ 8.40 (m, 1H, ArH), 7.84 (m, 10H, ArH), 7.64 (m, 24H, ArH), 7.44 (m, 11H, ArH), 4.23 (br, 4H, Cz-H), 2.12 (br, 20H), 1.80(br, 6H), 1.14(br, 74H), 0.8 (br, 50H, CH_3) ; ^{13}C NMR (75 MHz, $CDCl_3$) δ 151.81, 140.52, 140.02, 129.35, 128.80, 127.22, 126.16, 122.87, 122.56, 121.53, 119.99, 55.35, 40.41, 31.51, 31.49, 29.70, 23.86, 22.59, 14.10, 14.07, 14.04; M_n = 6.7 kDa; M_w = 21.2 kDa.

As for **P1**, 11% of **M1** were found to be inserted within the polymer backbone according to the ^{1}H NMR spectrum by comparing the intensity of the signal at 4.23 ppm attributed to Cz-H of **M2** with the intensity of the signal at 0.8 ppm attributed to the CH_3 protons of the fluorene hexyl chains.

Poly(9,9-dihexylfluorene-co-(phenyl-terpyridine) carbazole) (**P3**).

Yield 20%; ^{1}H NMR (300 MHz, $CDCl_3$, ppm) δ 8.87 (d, 2H), 8.75 (m, 6H), 8.56 (br, 2H), 8.23 (d, 2H), 7.84 (br, 76H), 7.69 (br, 150H), 7.47(m, 2H), 7.36(m, 2H), 2.08 (br, 160H), 1.15 (br, 542H), 0.81(br, 408H); ^{13}C NMR (75 MHz, $CDCl_3$, ppm) δ 151.81, 151.00, 149.22, 140.52, 140.02, 127.21, 126.16, 121.52, 119.98, 55.34, 40.39, 31.48, 29.69, 23.86, 22.58, 14.05; M_n = 8.4 kDa; M_w = 16.2 kDa.

The average molar ratio of **M3** within the polymer chain is calculated to be 3 % by comparing the integrated signals at 0.81 ppm attributed to the fluorene's CH_3 groups and at 8.87–8.70 ppm attributed to the terpyridine moiety.

Poly(9,9-dihexylfluorene-alt-(pyridine-benzo-imidazole) carbazole) (**P4**).

Yield 10%; ^{1}H NMR (300 MHz, $CDCl_3$, ppm) δ 8.60 – 8.02 (m, 4H), 7.88 – 7.56 (m, 7H), 7.55 – 6.78 (m, 7H), 4.80 (br, 2H, Cz-H), 4.31 (br, 2H, Cz-H), 2.27 – 1.75 (m, 8H), 1.42 (br, 8H), 1.10 (br, 12H), 0.77 (t, J = 6.7 Hz, 6H, CH_3); ^{13}C NMR (75 MHz, $CDCl_3$) δ 150.77, 150.65, 148.73, 147.58, 139.49, 139.30, 139.19, 138.98, 135.77, 135.45, 127.75, 127.53, 126.16, 125.12, 123.68, 122.72, 122.57, 122.30, 121.60, 120.48, 118.95, 109.12, 54.30, 44.23, 39.35, 30.46, 30.44, 28.65, 25.91, 25.64, 25.53, 22.82, 21.56, 21.54, 13.05, 13.01, 12.99; M_n = 3.1 kDa; M_w = 4.6 kDa.

The average amount of the carbazole moiety in the polymer chain is calculated to be 50% according to the ^{1}H NMR spectrum.

Poly(9,9-dihexylfluorene-alt-(phenyl-benzo-imidazole) carbazole) (**P5**).

Yield 12%; ^{1}H NMR (300 MHz, $CDCl_3$) δ 8.49 (s, 2H), 7.93 – 7.63 (m, 10H), 7.55 – 7.30 (m, 5H), 4.26 (d, J = 29.1 Hz, 4H, Cz-H), 2.15 (d, J = 13.0 Hz, 4H), 1.73 (d, J = 36.0 Hz, 3H), 1.12 (d, J = 7.3 Hz, 13H), 0.79 (q, J = 10.7, 6.8 Hz, 8H); ^{13}C NMR (75 MHz, $CDCl_3$) δ 151.9, 151.7, 148.8, 148.7, 140.5, 136.9, 133.2, 126.4, 124.7, 123.8, 123.3, 123.1, 122.6, 121.7, 120.3, 119.1, 109.5, 45.3, 40.6, 31.7, 28.9, 26.6, 24.0, 22.8, 22.6, 14.3, 14.1. M_n = 7.3 kDa; M_w = 16.9 kDa.

The average amount of the carbazole moiety in the polymer chain is calculated to be 44% according to the ^{1}H NMR spectrum.

Poly(9,9-dihexylfluorene-alt-(phenyl-terpyridine) carbazole) (**P6**).

Yield 30%; ^{1}H NMR (300 MHz, $CDCl_3$) δ 8.83 (d, 2H), 8.78–8.67 (m, 4H), 8.22 (d, J = 1.9 Hz, 2H), 8.17-8.12 (m, 2H), 7.91 (td, J = 7.7, 1.8, 2H), 7.77 (br, 2H, Ar), 7.69-7.63 (m, 2H), 7.61 (br, 4H, Ar), 7.55 (dd, J = 8.7, 1.9 Hz, 2H), 7.39 (ddd, J = 7.5, 4.8, 1.2 Hz, 2H), 7.33 (d, J = 8.7Hz, 2H), 2.08 (br, 4H, CH_2), 1.07 (br, 16H, CH_2), 0.73 (m, 6H, CH_3, CH_2); ^{13}C NMR (75 MHz, $CDCl_3$) δ 156.01, 151.78, 149.15, 140.62, 139.71, 137.10, 134.54, 129.04, 127.21,

124.04, 121.47, 118.95, 31.52, 30.98, 29.75, 22.62, 14.12. Not enough soluble for GPC measurement.

The average amount of the carbazole moiety in the polymer chain is calculated to be 50% according to the ^{1}H NMR spectrum.

2.3. Stoichiometry and binding constants determination

The stability and the stoichiometries of the complexes were determined by fluorescence titration as follows. A **M3** solution with a concentration of 5×10^{-7} M in THF:H_2O (50:50 v/v) whose pH was maintained neutral with NaOH and HCl was prepared. Increasing volumes of a solution containing the metal ions (5×10^{-5} M) and **M3** (5×10^{-7} M) were added and the emission intensity was monitored. These experimental conditions insured the measurements to be conducted at a constant ligand concentration. Solutions were thoroughly mixed for 1 min prior to measurement. Global analysis of the whole emission spectra was effectuated with the SPECFIT software (V3.0 for 32-bitWindows). This software uses singular value decomposition and non-linear regression modelling by the Levenberg–Marquardt method. [22, 23, 24]

2.4.Titration of monomers and polymers with calcium and metal ions

Polymer titrations were done by incremental addition of 5×10^{-4} M aqueous solutions of the ions to 2 ml of 5 μg/ml polymer solution in THF (the concentration of the metal ions in THF range from 1.2×10^{-6} M to 2.5×10^{-5} M). Measurements were conducted with fresh test solutions that were thoroughly mixed with the monomers or polymers solutions for 1 min before measurement. Aqueous solutions of $AlCl_3$, $CaCl_2$, $CdCl_2$, $CuSO_4$, $FeCl_2$, $FeCl_3$, $HgCl_2$, $MgCl_2$, $NiCl_2$ and $ZnCl_2$ were used.

The Stern-Volmer constants (K_{sv}) of the polymers were determined according to the equation

$$\frac{I_0\text{-}I}{I_0\text{-}I_f} = K_{sv}\,[\mathrm{Q}]$$

where I_0 and I are the maximum intensities without and with a quencher, respectively, I_f is the final intensity of the photoluminescence spectrum when equilibrium between the fluorophore and the quencher is reached, K_{sv} is the Stern-Volmer constant (quenching coefficient), and [Q] is the concentration of the quencher ions. In case the fluorescence is totally quenched ($I_f = 0$), the equation is simplified in: $\frac{I_0}{I} = 1 + K_{sv}[Q]$

2.5. Quantum yields determination

The photoluminescence quantum yields of the monomers were measured relatively to a solution of 1,4-bis(2,5-phenyloxazolyl)benzene in cyclohexane ($\Phi_{abs} = 0.93$), and that of the polymers were measured relatively to a solution of quinine sulphate in 0.1 M H_2SO_4 solution as reference at 295 K ($\Phi_{abs} = 0.54$). The following equation was used to calculate the quantum yields,

$$\frac{\Phi_x}{\Phi_r} = \frac{A_i Abs_r \eta^2_x}{A_x Abs_x \eta^2_r}$$

r refers to the reference and x to the sample, A_i is the area under the spectrum, Abs_i is the absorbance at the excitation wavelength, and η_i is the refractive index of the medium. [25]

1. Results and discussion

1.1. Synthesis

Monomers synthesis. Prior to polymer synthesis, the functionalized **M1**, **M2** and **M3** monomers were isolated. Their molecular structure and synthesis are depicted on the Scheme, as well as that of the intermediary products. **M1** and **M2** were isolated as follows: 2,7-dibromocarbazole was initially reacted with dibromohexane to yield **1** [8] which was further reacted with 2-(2-Pyridyl)benzimidazole and 2-Phenylbenzimidazole to afford **M1** [18] and **M2**, [19] respectively. Monomer **M3** was obtained from a 3-step procedure, which consisted in the synthesis of 4-(9H-carbazol-9-yl)benzaldehyde, [20] which was subsequently brominated

with *N*-bromosuccinimide. The resulting compound was reacted with 2-acetyl pyridine in the presence of ammonium hydroxide by Kröhnke-type condensation reactions to afford the desired **M3** monomer whose structure was probed with the help of NMR spectroscopy (see experimental part). [26]

Polymers synthesis. All polymers were synthesized *via* a Suzuki-Miyaura cross-coupling reaction in the conditions previously described. [8] For the synthesis of the random **P1**, **P3**, and **P5** polymers, 0.2 eqv. of each dibrominated monomer was initially introduced with 0.3 eqv. of 2,7-dibromo-9,9-dihexyl-9*H*-fluorene and 0.5 eqv. of 9,9-di-hexylfluorene-2,7-diboronic acid. NMR analysis showed that the polymers content of the carbazole-containing monomer amounts to 11% in **P1** and **P2**, and to only 3% in **P3.** It is lower than expected from the quantities of monomers used, which could arise either from the fact that increasing amounts of 3,6-carbazole in a poly(2,7-fluorene) backbone resulted in polymers with lower solubility, as previously observed, [8] or from the relatively low reactivity of the carbazole unit in the 3 and 6 positions associated to the steric hindrance of the pendant group. [27]

2.2.Optical properties of the monomers in presence of various cations

Three coordinating groups, namely 2-(2-pyridyl)benzimidazole, 2-phenylbenzimidazole, and 2,2′:6′,2″-Terpyridine, were attached to the polymer backbones in order to probe their ability to interact with different divalent and trivalent metal ions and evaluate whether selectivity towards complexation and cation recognition was effective. The spectroscopic data obtained for all compounds are reported in Table 1. The effect of the cations on the spectroscopic properties of the three monomers was then investigated in solution. It is described below.

Absorption spectra of **M1**, **M2**, and **M3**, and their solutions upon addition of an excess (12.5 eqv) of Al^{3+}, Ca^{2+}, Cd^{2+}, Cu^{2+}, Hg^{2+}, Mg^{2+}, Ni^{2+}, and Zn^{2+} in 50 µl of aqueous solutions are

shown in Figure 1a-c. The effect of the Fe^{2+} and Fe^{3+} ions was not investigated by absorption spectroscopy as they absorption interferes with that of the monomers (see Supporting information, Figure S1).

The spectrum of **M1** is, as expected, a combination of the absorption spectra of 2-(2-pyridyl)benzimidazole and carbazole as the two units are not conjugated. Three maxima at 273, 344 and 362 nm are the consequence of the absorption of the carbazole unit, while the absorption of the 2-(2-pyridyl)benzimidazole moiety appears as a band with a maximum at 304 nm and a shoulder at 320 nm. It shows no visible change after addition of an excess of Cd^{2+}, Hg^{2+}, Mg^{2+}, Al^{3+}, and Zn^{2+}, while an isosbestic point is located at 322 nm after addition of solutions of the Ni^{2+}, Cu^{2+}, and Ca^{2+} ions. This indicates that interaction between the monomer and these three cations occurred with formation of new species.

The interaction between **M1** and the Ni^{2+} and Cu^{2+} ions was confirmed by monitoring the emission of the monomer with an excess of metal ions (Figure 2a). Addition of 12.5 eqv of the metal ion resulted in a 60% and 35% quenching of the luminescence of **M1** with $NiCl_2$ and $CuSO_4$, respectively. As can be seen from Figure 2a, a loss of about 10% of the intensity was observed after addition of Ca^{2+}, which corresponds to dilution as it superimposes on the emission spectrum recorded after addition of the same volume of deionized water. The 50% decrease in the monomer emission was also observed with Fe^{2+} and Fe^{3+} solutions. However, it is mostly due to absorption of the salts (see Supporting information, Figure S1).

Same experiments were conducted with **M2** (Figures 1b and 2b). The absorption properties of **M2** are similar to that described above for **M1**. No noticeable change could be observed in the absorption spectra after addition of an excess of the Ca^{2+}, Cd^{2+}, Mg^{2+}, Cu^{2+}, Hg^{2+}, Ni^{2+}, and Zn^{2+} ions. The emission intensity was not either modified after addition of these ions. A decrease by 50% and 70% in the emission intensity was observed with the Fe^{2+} and Fe^{3+} ions, respectively. As for **M1**, we mainly attributed a 50% emission quenching to the absorption of

Fe^{2+} and Fe^{3+} solutions. Hence, we observed a 20% decrease in emission in the presence of the Fe^{3+} ion, and we also noticed a decrease by 20% of the initial **M2** emission in presence of the Al^{3+} ions. This suggests an interaction between **M2** and the Fe^{3+} and Al^{3+} ions.

The functionalization of **M3** is relatively different from that of **M1** and **M2**. The coordinating terpyridine group is connected to the carbazole unit *via* a phenyl ring, resulting in a conjugated system between the two moieties. This impacts the electronic properties of monomer **M3** and is the reason why the absorption spectrum is not a simple combination of the absorption spectra of the carbazole and terpyridine units. It shows maxima at 270, 292, 302, 318 and 355 nm with decreasing intensity in the range 250-400 nm (Figure 1c). The absorption spectrum of **M3** shows a significant change when the Ni^{2+}, Cd^{2+}, and Zn^{2+} ions are added and two isosbestic points at 288 and 325 nm are seen, while the structured spectrum disappeared with Cu^{2+}. Emission spectra of **M3** recorded after addition of the metallic solutions are reported on Figure 2c. They confirm the interaction of **M3** with these four metal ions. Addition of 12.5 eqv of Cu^{2+} and Ni^{2+} can even quench up to 90% of the monomer emission, and addition of 12.5 eqv of Fe^{2+} can quench it up to 95%. The effect of Cd^{2+} and Zn^{2+} is even more spectacular as the emission band showing a maximum at 410 nm disappeared and a new emission centered at 500 nm appeared with an *ca* 450% increase in intensity.

The stoichiometry of the complexes formed between **M3** and the Zn^{2+} and Ni^{2+} ion as well as their binding constants were determined. Monomer **M3** was chosen as the polymers comprising the terpyridyl unit were found to be highly sensitive to these two ions (see below).

The measurements described above indicate the possibility of interaction between the functional groups and some of the ions investigated. Table 2 summarizes the selectivity of the monomers towards the investigated metal ions. Comparison between the results obtained for **M1** and **M2** clearly shows the positive impact of the donor nitrogen atom on the coordination of the Ni^{2+}, Cu^{2+}, and Ca^{2+} ions when switching from a phenyl group (**M2**) to a pyridyl group

(**M1**). They particularly show that **M1** and **M3** are interesting candidates for designing more elaborated sensor materials as their emission is modified by several of the investigated ions. These three compounds were thus used to synthesize emissive conjugated polymers derived from polyfluorene.

2.3. Optical properties of the polymers

Random copolymers were obtained with a fluorene:carbazole monomer ratio of 9:1 for **P1** and **P2** with **M1** and **M2**, respectively, and a ratio of 9.7:0.3 for **P3** with **M3**. These ratios were determined by proton NMR spectroscopy. The corresponding alternating fluorene-*alt*-carbazole polymers, **P4**, **P5** and **P6** were also synthesized with **M1**, **M2**, and **M3**, respectively. The polymers structures are reported on the Scheme. For comparison, fluorescence titration measurements were also done with Poly(9,9-di-*n*-hexyl-2,7-fluorene (**PF**) to highlight the impact of the pendant functional groups on the polymers emission in the presence of the metal ions.

2.3.1 Photophysical properties of the polymers.

The spectroscopic data of the polymers are reported in Table 1. Absorption spectra are reported on Figure S2. They all show maxima in the near-UV region. The emission spectra of **PF** and **P1–P6** in THF are reported on Figure S3. The emission spectrum of **PF** showed a structured band with two maxima at 422 nm and 446 nm and a shoulder at 477 nm. Polymers **P1**–**P5** have a similar emission spectrum as **PF**. This indicates that emission of these polymers is mainly controlled by the fluorene segments present in the polymer backbones. **P6** shows a broad emission band centered at 450 nm. This is the consequence of the migration of electron density from the carbazole donor groups towards the terpyridyl acceptor, resulting in intramolecular charge transfer interactions and a bathochromic shift. [28]

2.3.2. Luminescence titrations.

The variation of **PF** emission intensity after addition of solutions of Al^{3+}, Ca^{2+}, Cd^{2+}, Cu^{2+}, Fe^{2+}, Fe^{3+}, Hg^{2+}, Mg^{2+}, Ni^{2+}, and Zn^{2+} is reported on Figure 3a. A slight decrease by 2-8% of the polymer emission was observed. To decorrelate this effect of a dilution effect, the same volumes of deionized water were added to the **PF** solution (black curve, Figure 3a). The decrease in emission did not exceed 8%. It is concluded that the effect of the analytes on **PF** emission is negligible as the decrease in intensity observed when the cations are added is similar to that obtained when the same volumes of deionized water are used. We have worked with highly diluted polymer solutions (5 μg/mL), thus, each macromolecule is considered isolated and no interaction occurs between it and other molecules as this concentration was found to be in the linear domain of the graph showing the concentration *vs* the emission intensity of **PF** (Figure S4).

The variation of **P1** emission intensity with concentrations of the ten ions ranging from 0 to 2.5 $\times 10^{-5}$ mol/L is shown on Figure 3b. It shows that, among the ions investigated, Cu^{2+} and Ni^{2+} ions have the most remarkable influence on the emission of **P1**. It decreases by up to 45 and 25% at saturation for the Cu^{2+} and Ni^{2+} ions, respectively, while the decrease in the emission intensity is comprised in the range 5-12% in presence of the other metal ions. We define saturation as being the concentration at which the intensity of the polymer emission does not decrease significantly anymore upon further addition of the metallic solution. A decrease in polymer emission by *ca* 20% was also observed with the Fe^{2+} and Fe^{3+} ions, which is about 10% more than with the other ions beside Cu^{2+} and Ni^{2+}. This 10% additional decrease in emission is the consequence of the absorption of the salts. Figure 3b shows that emission spectroscopy is suitable to selectively detect the Cu^{2+} and Ni^{2+} ions with **P1**.

The same titrations were performed with **P2**. They are reported on Figure 3c. Variations between 3 and 10% of the initial polymer intensity were obtained. Even though **M2** emission

was found to be impacted by the Al^{3+} and Fe^{3+} ions, the fluorescence of **P2** was not remarkably altered by these two ions in the investigated concentration range. These results lead to the conclusion that **P2** is not suitable for sensing these ions with a satisfying sensitivity. They show that changing a pyridine moiety for a phenyl group does not bring any selectivity and is particularly detrimental to the detection of the Cu^{2+} and Ni^{2+} ions. This corroborates the study of the monomers presented above which were found to be not sensitive to these ions.

Several conjugated polymers comprising the terpyridyl groups as pendant coordination sites and conjugated with the polymer backbone were recently reported as optical sensing elements. A high sensitivity towards Cu^{2+}, [26] Ni^{2+}, [29] Fe^{3+}, [30, 31] or Zn^{2+} [32] could be found. The selectivity was strongly related to the backbone structure. [30] Taking these findings into account, we designed the random polymer **P3**. Remarkable changes were obtained with **P3** for which the coordinating groups were linked to the polymer backbone *via* a phenyl moieties. Figure 3d shows that a significant decrease in the luminescence intensity of **P3** was observed after addition of the Zn^{2+} (23%), Fe^{2+} (18%), Ca^{2+} (20%), Ni^{2+} (24%), Cu^{2+} (25%), and Al^{3+} (25%) ions. The percentages indicated in parentheses refer to the decrease in intensity. The sensitivity of **P3** luminescence to the Zn^{2+}, Ni^{2+} and Cu^{2+} ions was expected as the optical properties of the monomer **M3** were found to be impacted by these ions as described above.

The alternating fluorene-*alt*-carbazole polymers **P4**, **P5**, and **P6** were synthesized with **M1**, **M2**, and **M3**, respectively. The goals were both to introduce a highest amount of the functional monomers and to evaluate the influence on the photophysical properties of the polymers brought by the backbone structural change. Indeed, the regular alternation of carbazole and fluorene units within the polymers chain was expected to modify the position of the energy levels of the excited states with respect to their random counterparts. These changes were thus anticipated to increase (with more binding sites per polymer chain) or modify the sensitivity of the polymers and, to some extent, tune their sensing properties.

Titrations were performed with **P4**, **P5**, and **P6** in a similar way than described for their random counterparts. Results are reported on Figures 3e-g for **P4, P5**, and **P6**, respectively. When switching from **P1** to **P4**, the quenching efficiency caused by the metal ions is more remarkable. The emission of **P4** dropped down by *ca* 80% of the initial value after addition of 2×10^{-5} M solutions of Cu^{2+} and Ni^{2+} with saturation reached for Ni^{2+} and saturation almost reached for Cu^{2+}. The decrease in intensity that was previously obtained for **P1** with the same amounts of Ni^{2+} and Cu^{2+} ions was only 30 and 45 %, respectively. This shows that an improvement of the sensitivity was obtained with **P4**. Also, it can clearly be seen that saturation is obtained for a Ni^{2+} concentration of 1×10^{-5} M, while it was obtained at approximately 2.5×10^{-6} M with **P1**. This corresponds to the 4-fold increase of the functionalized carbazole when going from **P1** to **P4**. Thus, **P4** is saturated at a higher concentration of metal ions, and this is attributed to the higher quantity of coordinating sites. In addition, sensitivity of **P4** to the Ca^{2+} and Al^{3+} ions was also observed. The polymer emission intensity decreased down to *ca* 40% for Al^{3+} and 50% for Ca^{2+} of its initial value when saturation is reached. This sensitivity to Ca^{2+} is consistent with the absorption spectrum of **M1** that was modified by the presence of Ca^{2+} ions. The sensitivity of **P4** to Cu^{2+} is in contrast with a previous report on a similar alternating polymer bearing octyl chains branched on the fluorene units for which the luminescence was found to be hardly quenched by Cu^{2+} at a concentration of 1×10^{-4} M. [18] Saturation was reached for Ni^{2+} and Cu^{2+} at 2.5×10^{-5} M, however it was not reached for Ca^{2+} and Al^{3+}. This difference is due to the complexation reaction kinetics between the polymer and the different ions and results from the fact that **P4** complexes some metal ions in a time-dependent way as described hereafter. The emission intensity of **P4** was monitored over time after addition of 1.25×10^{-5} M of $CuSO_4$, $AlCl_3$, and $CaCl_2$. Spectra were recorded every 5 min in a 0–15 min period for the Cu^{2+} and Ca^{2+} ions and in a 0–60 min period for the Al^{3+} ion (Figure S5). They show that luminescence quenching occurred immediately after addition of the Cu^{2+} ion, while the emission of **P4**

decreased progressively for the Ca^{2+} and Al^{3+} ions, confirming a kinetic effect with these two ions.

No significant change was observed with **P5** with respect to **P2**, confirming the inability of the phenyl-benzimidazole group to interact efficiently with the investigated ions.

The emission spectra of **P6** in presence of the ions are shown on Figure 4 (Top). **P6** emission was more efficiently quenched with respect to the corresponding random **P3** polymer. The luminescence was almost totally quenched with the Ni^{2+}, Zn^{2+}, Cu^{2+} and Cd^{2+} ions, while it dropped down to 10 % (Fe^{2+}), 14% (Al^{3+}, Ca^{2+}), and 41% (Fe^{3+}) of its initial intensity. Here also, these results contrast with a recent report with poly(metaphenylene-*alt*-fluorene) whose luminescence was hardly quenched by the Cu^{2+}, Zn^{2+}, and Cd^{2+} ions, and confirm the importance of the structure of the conjugated backbone. [26] No significant decrease in the polymer emission was observed for the Mg^{2+} and Hg^{2+} ions. Remarkably, the formation of a complex between the Zn^{2+} ions and **P6** was highlighted by the presence of a new band centred at 585 nm. This is commonly observed with conjugated polymers bearing terpyridyl groups, [12,29,33,34] as coordination of the Zn^{2+} ion results in a facilitated intramolecular charge transfer from carbazole to the terpyridyl unit. [35] A similar result was observed with Cd^{2+}, as an emission band centred at 585 nm also appeared. Quenching of the band centred at 450 nm and occurrence of the band at 585 nm makes possible a discrimination of the Zn^{2+} and Cd^{2+} ions from the other ions. This is an important point in view of elaborating selective optical sensors, and this will be emphasized in the "*competitive titrations*" part. Pictures of **P6** solutions containing the ions taken under UV light show that the Zn^{2+} and Cd^{2+} ions can be detected by the eye, even at low concentration (Fig. 4b).

The results described hereabove also show that, as a general trend, the selectivity lowers when going from the polymers with the lowest coordinating group content to the polymer with the highest amount of the functionalized carbazole. This is emphasized in Table 3.

2.3.3. Quenching efficiency

The efficiency with which the emission is quenched was investigated by determining the Stern-Volmer quenching constants and the limits of detection (LOD) when possible. The Stern-Volmer constants of the polymers were determined by calculating the slope of the curve with the equation I_0-I/I-I_f = K_{sv} [M^{x+}] in the linear domains at lowest metal ions concentration. [36] An example of the Stern-Volmer plot resulting from the titration of **P6** with Zn^{2+} is shown on Figure 5. Table 4 summarizes K_{SV} for **P1**, **P3**, **P4** and **P6** towards different metal ions.

The K_{sv} values are representative of the efficiency with which the emission of each polymer is quenched. It can be seen that **P1**, **P3**, **P4** and **P6** have the highest K_{SV} towards Ni^{2+}, with values in the order of 10^6 M^{-1}. They are relatively high as values in the range 10^4–10^5 are generally reported for similar systems. [26, 29, 31, 32, 35, 37] This indicates that the four polymers possess a satisfying quenching efficiency towards Ni^{2+}. Besides Ni^{2+}, **P3** and **P6** show K_{SV} values of 9×10^5 M^{-1} with Cu^{2+} and Zn^{2+}, suggesting an efficient quenching efficiency of these two ions towards these two polymers. **P1** and **P4** show K_{SV} towards Ni^{2+} in the same order of magnitude (2.1×10^6 and 2.0×10^6 M^{-1} for **P1** and **P4**, respectively) and values of 3.0×10^5 M^{-1} and 5.4×10^5 M^{-1} were determined for the Cu^{2+} ion for **P1** and **P4**, respectively). These values show that the Stern-Volmer constants of the polymers are independent from the amount of ligand in the polymer backbone, hence the polymer backbone structure. This is confirmed by the values found for **P3** and **P6** towards Ni^{2+}, Cu^{2+} and Zn^{2+}.

The limits of detection could be estimated according to the equation LOD = 3 × Sb_1/K_{sv}, where Sb_1 is the standard deviation of the blank solution (2% in the present study). [38] They are reported in Table 5. The lowest LODs were obtained for the Ni^{2+} ion which showed the highest Stern-Volmer constants. Values lower that 2 ppb were obtained with **P1**, **P3, P4** and **P6**. The LOD of **P3** and **P6** towards Cu^{2+} and Zn^{2+} were found to be lower than 5 ppb.

2.3.4. Competitive titrations

The studies reported above revealed that the emission of **P1** was only influenced by the Ni^{2+} and Cu^{2+} ions, and that **P6** showed a new emission band only in the presence of the Zn^{2+} and Cd^{2+} ions. This indicates that these two polymers are promising candidates for elaborating selective optical sensors. Competitive titrations were thus performed with **P1** and **P6** with the aim of investigating if any selectivity could be emphasized.

A solution containing $CdCl_2$, $HgCl_2$, $ZnCl_2$, and $CaCl_2$, each at a concentration of 5×10^{-4} M, was used. For each of the Ni^{2+} and Cu^{2+} ions, for which the highest Stern-Volmer constants were found with **P1**, two types of experiments were performed. They are reported on Figure 6. First, 50 µl of deionized water was added to a 2 mL solution of **P1**. This lead to a very slight decrease of 4% in the polymer emission intensity, due to dilution effect. Then 50 µl of a 5×10^{-4} M solution of the Cu^{2+} ion was added. The intensity dropped down to 56 % of the initial value. In a second experiment, 50 µl of the solution containing the Cd^{2+}, Hg^{2+}, Zn^{2+} and Ca^{2+} ions was firstly added to the solution of **P1**. Only a slight decrease in intensity was observed, similar to that obtained by dilution effect. Then, the Cu^{2+} solution was added, resulting in a 31% decrease in emission intensity of the initial value.

The two same experiments were conducted with the Ni^{2+} ion. After addition of water, followed by addition of the Ni^{2+} solution, the intensity decreased by 21% of the initial value. Addition of the mixture solution to **P1**, followed by addition of the Ni^{2+} solution resulted in a 19% decrease of the emission intensity, which is, within experimental error, similar to that obtained after addition of water. This shows that the four metal ions used in the mixture solution do not compete with the Ni^{2+} ion, as the intensity of emission obtained using the Ni^{2+} ion is the same with or without the presence of the mixture solution. We conclude that the quenching effect due to the presence of the Ni^{2+} ion is not altered by the presence of other metal ions, while a disruption in the effect of the Cu^{2+} ion on the emission of **P1** is observed in the presence of other metal cations. This indicates that a competition occurs between Cu^{2+} and the other metal

ions, and confirms that coordination of the Ni^{2+} ion is stronger than that with the other cations. This is an interesting point in view of using **P1** to elaborate selective optical nickel sensors.

In order to take advantage of the new emission band appearing when Zn^{2+} and Cd^{2+} are added to a solution of **P6** and to probe if the presence of other metal ions could interfere to the detection of these two ions, we have investigated the effect of other metal ions on the emission of **P6** solutions containing the Zn^{2+} or Cd^{2+} ions. These measurements are reported on Figure 7. In a first experiment, emission spectra of solutions of **P6** containing the Al^{3+}, Ca^{2+}, Cu^{2+}, Fe^{2+}, Fe^{3+}, Hg^{2+}, Mg^{2+}, and Ni^{2+} ions, were recorded (Figure 7 a). Then, a solution of Zn^{2+} was added to each solution (Figure 7b). The emission band centered at 585 nm appeared in all solutions with a total quenching of the initial polymer emission, showing that the Zn^{2+} ion was able to displace the other cations. This is in accordance with the value of $10^{6.45}$ found for the association constant of the **[**Zn**M3]**$^{2+}$ complex compared to that of $10^{5.22}$ found for the **[**Ni**M3]**$^{2+}$ complex. In a second experiment, solutions containing an equivalent mixture of Cd^{2+} and one of the other cations was added to a solution of **P6** (Figure 7c). In all cases, the new band centered at 585 nm appeared and the initial **P6** emission at 450 nm dramatically dropped down. The two experiments described on Figure 7 clearly demonstrate that the presence of other metal ions does not hinder the qualitative detection of the Zn^{2+} and Cd^{2+} ions by **P6**. This is an important point in view of using **P6** as a selective sensor for these two cations.

2.3.5. Recyclability and solid-state sensors

Recyclability is a mandatory property for a non-disposable sensor. In order to have a clue on the possibility to regenerate and re-use a solution of **P1** for Ni^{2+} sensing, we have performed the following experiment whose results are reported on Figure 8a. A Ni^{2+} ion solution was added to a solution of **P1**. When saturation was reached, about 21% of the initial polymer intensity was observed. Then, addition of an $EDTA^{4-}$ solution resulted in an increase of the polymer emission, showing that complexes formed between the Ni^{2+} ions and $EDTA^{4-}$ are more

stable than the polymer-Ni complexes. A second addition of the Ni^{2+} solution again resulted in a loss of *ca* 20% of the polymer emission. Four cycles were performed, and the ratio between the polymer emission before and after addition of the Ni^{2+} solution was always around 20%. This experiment shows that no loss in the quenching efficiency of the Ni^{2+} ion on **P1** emission could be observed and finally proved the recyclability of this optical sensor.

Experiments on the regeneration of the solutions have a limited interest, especially when quantitative data are needed, as the presence of complexes in solution and a possible excess of EDTA used to regenerate the solutions will firstly react with the next solutions of cations and pervert the titration results. We have then investigated the ability of the polymers to design solid-state sensors which are also easier to handle and to use in such repeating experiments.

A thin film of **P1** was spin-coated on a glass substrate from a 1,2-dichlorobenzene solution (8 mg/mL) and dried for 6 hours at 100°C prior to titration. The film was immersed into a 1.25×10^{-3} M solution of $CuSO_4$. Its emission intensity decreased down to *ca* half of its initial value, showing that the polymer film interacts with the Cu^{2+} ions. After immersion of this film in an EDTA solution, and rinsing with deionized water, the overall intensity of the starting **P1** film was recovered. This indicates that the Cu^{2+} ions coordinated to the polymer were de-complexed. A second immersion of the film in the $CuSO_4$ solution resulted in a decrease of about 40% of the emission of **P1**. This sequence undoubtedly shows the recyclability of such an optical sensor. It is shown on Figure 9.

2. Conclusions

We have reported two series of emissive conjugated polymers comprising the fluorene and carbazole motifs in the backbone. The first series consists of three random copolymers and the second series comprises three alternating polymers. Three coordinating groups were attached as pendant units to the carbazole moieties, namely 2-(2-Pyridyl)benzimidazole, 2-

Phenylbenzimidazole, and terpyridine. These polymers have been investigated as optical sensing elements to probe the presence of calcium and metal ions of importance in biology and for environmental issues. Our investigations have shown that polymers comprising the 2-Phenylbenzimidazole moiety were not suitable to optically sense the investigated cations. This was attributed to an inefficient coordination of the cations to the 2-Phenylbenzimidazole group. It was found that 2-(Pyridyl)benzimidazole was well-suited to probe the Ni^{2+} ion with an interesting selectivity. The emission of **P1** was also shown to be relatively sensitive to Cu^{2+} ions. **P4** emission dropped down by *ca.* 80% of its initial intensity with the Ni^{2+} and Cu^{2+} ions, while the decrease was about 30 and 50% with **P1**, respectively. Furthermore, the luminescence of **P4** was also efficiently quenched by the Ca^{2+} and Al^{3+} ions. Sensing of the Ca^{2+} ion is of interest in view of assessing the hardness of water. The luminescence of **P3**, was found to be moderately sensitive to the Cu^{2+}, Ni^{2+}, Al^{3+}, Ca^{2+} and Zn^{2+} ions with a maximum 25%-quenching of the emission intensity. However, the corresponding alternating polymer (**P6**) showed an increased sensitivity to several cations. In particular, the emission of **P6** was almost totally quenched by the Ni^{2+}, Zn^{2+}, and Cu^{2+} ions. The presence of Zn^{2+} and Cd^{2+} ions has the additional effect to raise a new emission band which is red-shifted compared to **P6**, paving the way to the elaboration of selective zinc or cadmium optical sensors. The possibility to elaborate selective sensors for the Zn^{2+} and Cd^{2+} ions is further reinforced by the results of competitive titrations. If the terpyridine group had already been reported to yield polyfluorene derivatives optically sensitive to the Zn^{2+}, Fe^{3+}, Zn^{2+}, and Cu^{2+} ions, it had never been shown that it could yield polymers sensitive to the Cd^{2+} ion, which is among the most toxic metal ions. Finally, **P6** showed a good sensitivity towards metal ions as it can detect Ni^{2+} and Zn^{2+} down to 2 ppb and 4 ppb, respectively.

Our conclusions, along with comparison with other polyfluorene-based conjugated polymers reported in the literature, confirmed that both the coordinating group and the conjugated

backbone have to be carefully taken into consideration for the design of optical sensors with conjugated polymers. For instance, the terpyridine moiety was described to give the best sensitivity for the Fe^{3+}, [30, 33, 38] or Ni^{2+} [28,34] ions, depending on the polymer backbone. Our study showed that a small amount of ligand already guarantees a significant quenching of the polymer emission. Also, the relationship between the selectivity of the polymer and the quantity of the attached coordinating groups acting as the probe was highlighted for the first time. The same coordinating group can lead to different sensitivity and selectivity with the same analyte depending on the backbone structure.

Acknowledgements

We wish to thank Dr Laurent Bouteiller for a facilitated access to the GPC equipment. Ecole polytechnique and CNRS are acknowledged for their financial support. XW thanks LabEx CHARMMMAT (ANR-11-LABEX-0039) for a PhD grant, QL thanks the China Scholarship Council for a PhD fellowship, and SR thanks the EU for a postdoctoral grant (Grant agreement 644852).

Supplementary data

Absorption of the salt solutions, emission spectra of **PF**, **P1**-**P6** in THF, emission intensity of **PF** versus concentration, emission spectra of **P4** *versus* time in presence of solutions of Cu^{2+} (left), Al^{3+} (middle), and Ca^{2+} (right) ions, and emission spectra of **P6** in presence of solutions of other metal ions are provided as Supplementary Material.

References

[1] J. Liu, G. Liu, L. Zang, W. Liu, Microchim. Acta 182 (2015) 547–555.

[2] H. N. Kim, W. X. Ren, J. S. Kim, J. Yoon, Coord. Chem. Rev. 41 (2012) 3210–3244.

[3] K.J. Barnham, C.L. Masters, A.L. Bush, Nat. Rev. Drug Discov. 3 (2004) 205–214.

[4] Y.H. Hung, A.I. Bush, R.A. Cherny, J. Biol. Inorg. Chem. 15 (2010) 61–76.

[5] J.C. Lee, H.B. Gray, J.R. Winkler, J. Am. Chem. Soc. 130 (2008) 6898–6899.

[6] Y. Zhang, Z.-W. Zhang, Y-M. Xie, S.-S Wang, Q.-H. Qiu, Y.-L. Zhou, G.-H. Zeng, Mol. Med. Rep. 12 (2015) 3273–3278.

[7] C.-Y. Chen, Y.-F. Wang, W.-R. Huang, Y.-T. Huang, Toxicol. Appl. Pharmacol. 189 (2003) 153–159.

[8] A. Sergent, G. Zucchi, R. B. Pansu, M. Chaigneau, B. Geffroy, D. Tondelier, M. Ephritikhine, J. Mater. Chem. C 1 (2013) 3207–3216.

[9] Q. Z. Zhou, T. M. Swager, J. Am. Chem. Soc. 117 (1995) 12593–12602.

[10] X.-H. Zhou, J.-C. Yan, J. Pei, Macromolecules 37 (2004) 7078–7080.

[11] V. Ibrahimova, M. E. Kocak, A. M. Onal, D. Tuncel, J. Polym. Sci. Part A Polym. Chem. 51 (2013) 815–823.

[12] M. Kimura, T. Horai, K. Hanabusa, H. Shira, Adv. Mater. 10 (1998) 459–462.

[13] X. Lou, Y. Zhang, S. Li, D. Ou, Z. Wan, J. Qin ; Z. Li, Polym. Chem. 3 (2012) 1446–1452.

[14] S.M Fonseca, R.P. Galvao, H.D. Burrows, U. Scherf, G.C. Bazan, Macromol. Rapid. Commun. 3 (2013) 717–722.

[15] Y. Qu, J.L. Hua, Y.H. Jiang, J. Polym. Sci. Part A Polym. Chem. 47 (2009) 1544–1552.

[16] Y.-J. Zhao, K. Miao, Z. Zhu, L.-. Fan, ACS Sens. 2 (2017) 842–847.

[17] Z.-B. Zhang, M. Fujiki, H.-Z. Tang, M. Motonaga, K. Torimitsu, Macromolecules 35 (2002) 1988–1990.

[18] B. Du, R. Liu, Y. Zhang, W. Yang, W. Sun, M. Sun, J. Peng, Y. Cao, Polymer 48 (2007) 1245–1254.

[19] H. Xu, D.-H. Yu, L.-L. Liu, P.-F. Yan, L.-W. Jia, G.-M. Li, Z.-Y. Yue, J. Phys. Chem. B 114 (2010) 141–150.

[20] T. Yu, H. Chai, Y. Zhao, C. Zhang, P. Liu, D. Fan, Spectr. Chim. Acta A: Mol. Biomol. Spectr. 209 (2013) 179–185.

[21] M. Sigalov, A. Ben-Asuly, L. Shapiro, A. Ellern, V. Khodorkovsky, Tetrahedron Lett. 41 (2000) 8573–8576.

[22] H. Gampp, M. Maeder, C. J. Meyer and A. D. Zuberbuhler, Talanta 32 (1985) 95–101.

[23] M. Brzeziński, T. Biela, Macromolecules 48 (2015) 2994–3004.

[24] X.Q. Pham, L. Jonusauskaite, A. Depauw, N. Kumar, J.P. Lefevre, A. Perrier, M.-H. Ha-Ti, I. Leray, J. Photochem. Photobiol. A : Chem. (364) 2018 355–362.

[25] A.M. Brouwer, Pure Appl. Chem. (83) 2001 2213–2228.

[26] A. Sil, N. Islam, S.K. Patra, Sensors Actuators B 254 (2018) 618–628.

[27] Name Reaction for homologation (2009) Part 1, Eds. J.J. Li and E.J. Corey.

[28] P. Leriche, A. Frère, A. Cravino, O. Alévêque, J. Roncali, J. Org. Chem. 72 (2007) 8332–8336.

[29] P.-C. Yang, H. Wu, H.-W. Wen, W.-N. Hung, Eur. Polym. J. 49 (2013) 2303–2315.

[30] Y. Cui, Q. Chen, D.-D. Zhang, J. Cao, B.-H. Han, J. Polym. Sci. Part A Polym. Chem. 48 (2010) 1310–1316.

[31] P.-C. Yang, S-Q. Li, Y.-H. Chien, T.-L. Tao, R.-Y. Huang, H.-Yu Chen, Polymers 9 (2017) 427–443.

[32] A. R. Rabindranath, A. Maier, M. Schäfer, B. Tieke, Macromol. Chem. Phys. 210 (2009) 659–668.

[33] C.-J. Cho, S.-T. Lu, C.-C. Kuo, F.-C. Liang, B.-Y. Chen, C.-C. Chu, React. Func. Polym. 93 (2015) 130–137.

[34] P.-C. Yang, H.-W. Wen, C.-W. Huang, Y.-N. Zhu, RSC Adv. 6 (2016) 87680–87689.

[35] P.-C. Yang, H. Wu, C.-L. Lee, W.-C. Chen, H.-J. He, M.-T. Chen, Polymer 54 (2013) 1080–1090.

[36] J.R. Lakowicz, Principles of Fluorescence Spectroscopy (2009), Springer, 3rd Edn.

[37] R.S. Juang, H.-W. Wen, M.-T. Chen, P.-C. Yang, Sensors Actuators B 231 (2016) 399–411.

[38] X. Bai, Y. Li, H. Gu, Z. Hua, RSC Adv. 5 (2015) 77217–77226.

Optical chemosensors for metal ions in aqueous medium with polyfluorene derivatives: sensitivity, selectivity and regeneration

Xinyang Wang,[a] Qiqiao Lin,[a] Sasikumar Ramachandran,[a] Gaëlle Pembouong,[b] Robert B. Pansu,[c] Isabelle Leray,[c] Bérengère Lebental, [a,d] Gaël Zucchi*[a]

Figure captions

Scheme. i) NaOH, DMF, 2-(2-Pyridyl)benzimidazole or 2-Phenylbenzimidazole; ii) K_2CO_3, DMF, CuI/Phen, 18C6; iii) NBS, DMF; iv) KOH, NH_4OH, EtOH, 1,4-dioxane, 2-Acetylpyridine; v) a) Tri(*p*-tolyl)phosphine, $Pd(OAc)_2$, TEAH, 9,9-di-*n*-hexylfluorene-2,7-diboronic acid bis(pinacol) ester, b) bromobenzene, c) phenylboronic acid pinacol ester.

Fig. 1. a) Absorption spectra of **M1**; b) **M2**; and c) **M3** (10^{-5} M in THF) in presence of 12. 5 eqv of various metal ions.

Fig. 2. a) Emission spectra of **M1**; b) **M2**; and c) **M3** (10^{-5} M in THF) in presence of 12.5 eqv of various metal ions (λ_{exc} = 305 nm for **M1** and **M2**, λ_{exc} = 330 nm for **M3**). * Intensities are given relatively to that of the monomer which was normalized.

Fig. 3. I/I_0 of 5 μg/mL THF solutions of a) **PF**; b) **P1**; c) **P2**; d) **P3**; e) **P4**; f) **P5**; g) **P6** upon addition of different volumes of $5 \cdot 10^{-4}$ M solutions of metal ions; I_0 is the intensity of the polymer solution before addition of the metal ions; λ_{exc} = 380 nm for **PF**, **P1**, **P2**, **P3**; λ_{exc} = 360 nm for **P4, P5**, **P6**; $V(M^{x+})$ is the added volume of the metal ion solution.

Fig. 4. Top: Emission spectra of **P6** in THF (5 μg/mL) in presence of the metal ions; bottom: corresponding photographs taken under illumination with 366-nm UV light.

Fig. 5. a) Left: Emission spectrum of **P6** (5 µg/mL in THF, λ_{exc} = 360 nm) upon addition of increasing amounts of Zn^{2+} ions; right: Stern-Volmer plot of **P6** versus Zn^{2+}. The blue curve indicates the domain that was taken in consideration to calculate K_{SV}.

Fig.6. Competitive titrations of **P1** with Cu^{2+} and Ni^{2+} and a mixture of Cd^{2+}, Hg^{2+}, Zn^{2+} and Ca^{2+}.

Fig. 7. a) emission spectrum of **P6** (5 µg/mL in THF, λ_{exc} = 360 nm) in presence of the Al^{3+}, Ca^{2+}, Cu^{2+}, Fe^{2+}, Fe^{3+}, Hg^{2+}, Mg^{2+}, and Ni^{2+} ions; b) emission spectra of **P6** in presence of equimolar amounts of Zn^{2+} and the Al^{3+}, Ca^{2+}, Cu^{2+}, Fe^{2+}, Fe^{3+}, Hg^{2+}, Mg^{2+}, and Ni^{2+} ions; c) emission spectra of **P6** in presence of equimolar amounts of Cd^{2+} and the Al^{3+}, Ca^{2+}, Cu^{2+}, Fe^{2+}, Fe^{3+}, Hg^{2+}, Mg^{2+}, and Ni^{2+} ions.

Fig. 8. I/I_0 of **P1** in presence of Ni^{2+} ions before and after addition of EDTA (4 cycles);

Fig. 9. Recyclability of an optical solid state sensor made with **P1**: right: emission spectra (λ_{exc} = 380 nm) in presence of the Al^{3+}, Ca^{2+}, Cu^{2+}, Fe^{2+}, Fe^{3+}, Hg^{2+}, Mg^{2+}, and Ni^{2+} ions of a thin film of **P1** before (1) and after (2) immersion in a Cu^{2+} solution; left: emission spectra of the same film after immersion in EDTA and rinsing with water (3) and after a second immersion in Cu^{2+} (4).

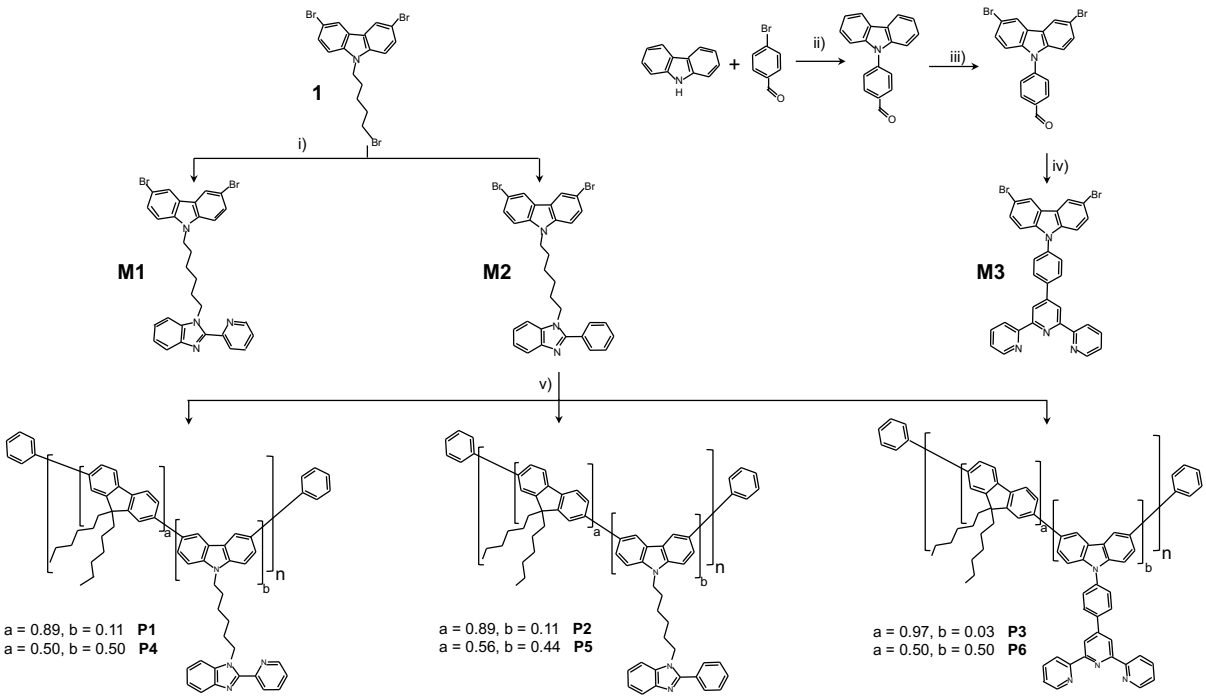
1
i)
ii)
iii)
iv)
v)
M1
M2
M3
a = 0.89, b = 0.11 P1
a = 0.50, b = 0.50 P4
a = 0.89, b = 0.11 P2
a = 0.56, b = 0.44 P5
a = 0.97, b = 0.03 P3
a = 0.50, b = 0.50 P6

Scheme

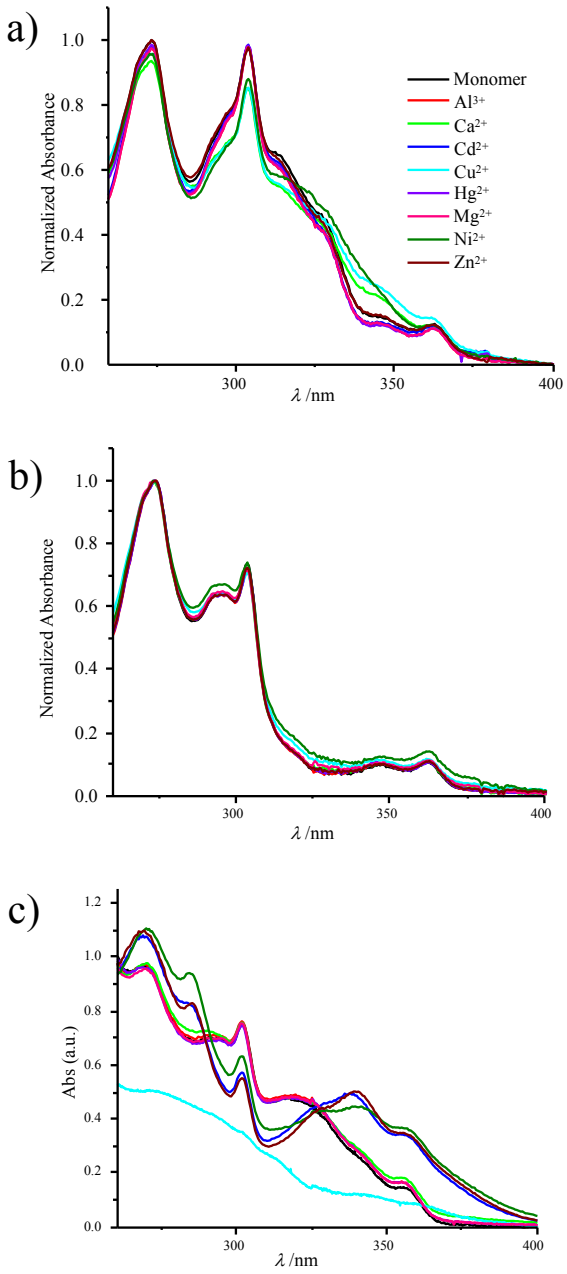
a)
Normalized Absorbance
λ /nm
Monomer
Al3+
Ca2+
Cd2+
Cu2+
Hg2+
Mg2+
Ni2+
Zn2+
b)
Normalized Absorbance
λ /nm
c)
Abs (a.u.)
λ /nm

Fig.1

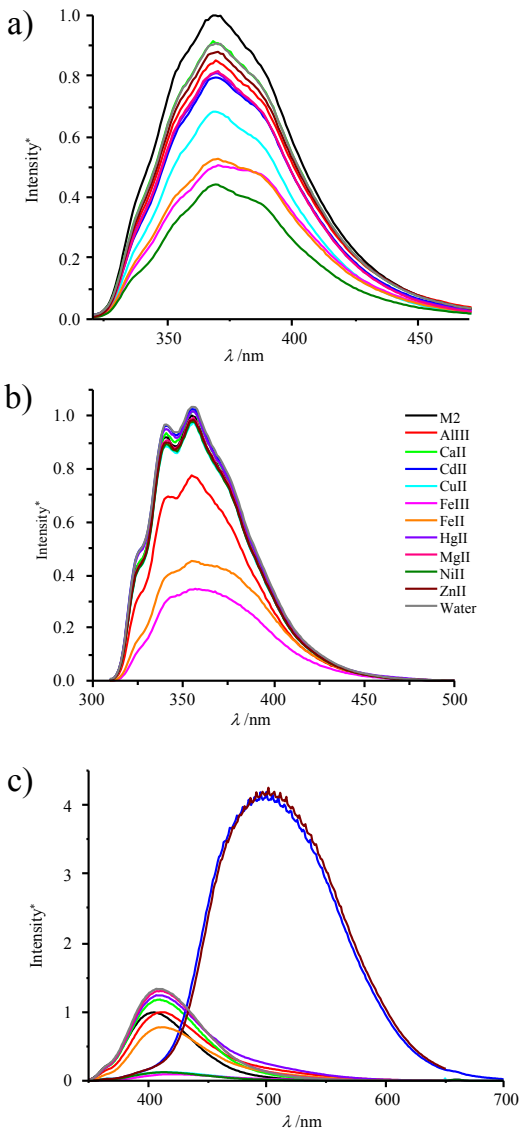
a)
Intensity*
λ /nm
b)
Intensity*
λ /nm
M2
AlIII
CaII
CdII
CuII
FeIII
FeII
HgII
MgII
NiII
ZnII
Water
c)
Intensity*
λ /nm

Fig. 2

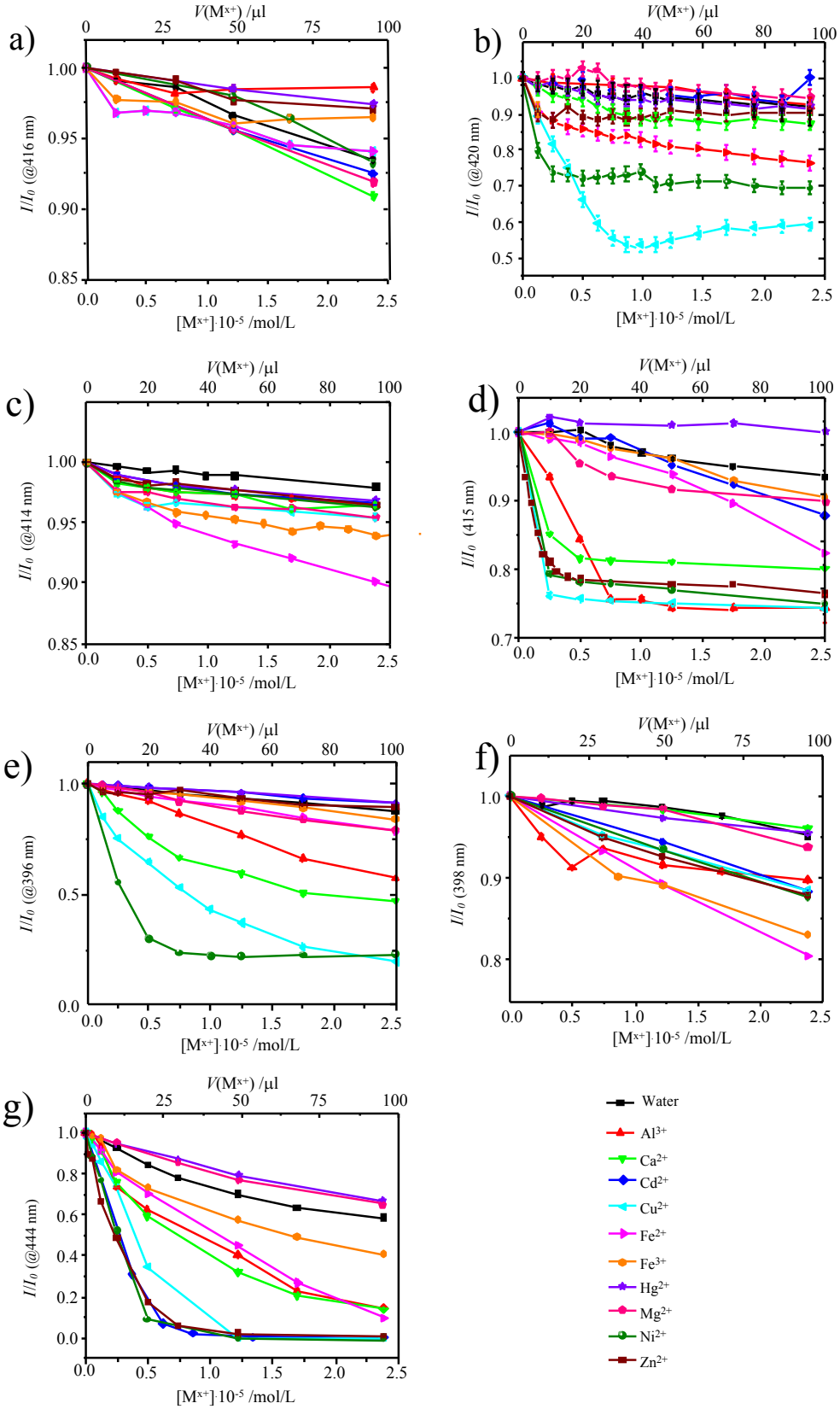
a)
b)
c)
d)
e)
f)
g)
V(Mx+) /μl
I/I0 (@416 nm)
I/I0 (@420 nm)
I/I0 (@414 nm)
I/I0 (415 nm)
I/I0 (@396 nm)
I/I0 (398 nm)
I/I0 (@444 nm)
[Mx+]·10-5 /mol/L
Water
Al3+
Ca2+
Cd2+
Cu2+
Fe2+
Fe3+
Hg2+
Mg2+
Ni2+
Zn2+

Fig. 3

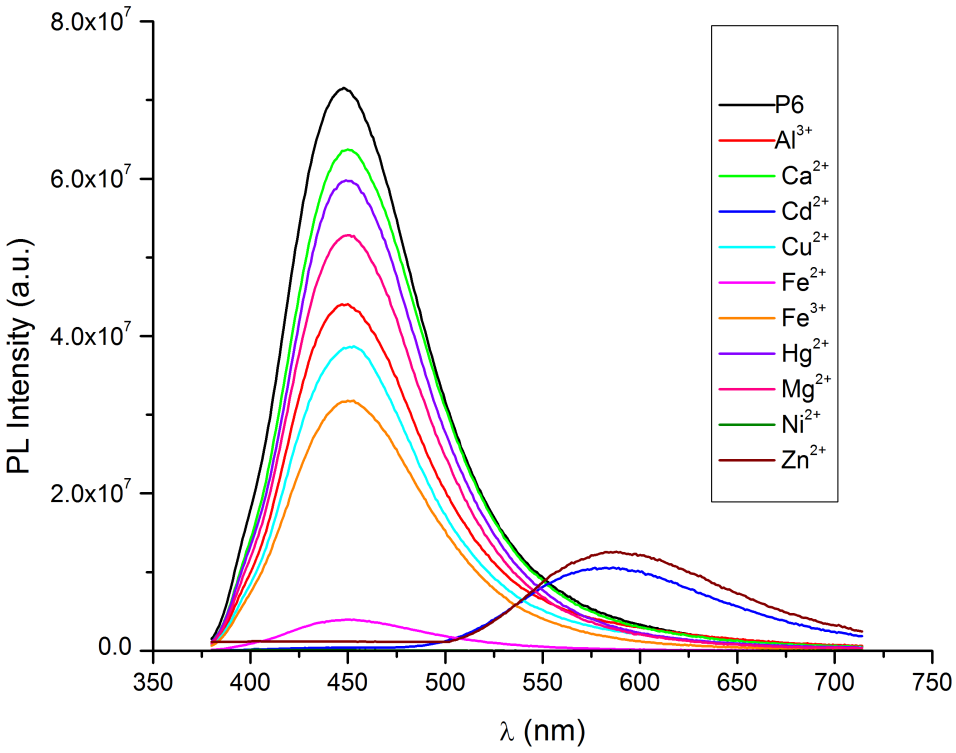
8.0x10^7
6.0x10^7
4.0x10^7
2.0x10^7
0.0
PL Intensity (a.u.)
350
400
450
500
550
600
650
700
750
λ (nm)
P6
Al3+
Ca2+
Cd2+
Cu2+
Fe2+
Fe3+
Hg2+
Mg2+
Ni2+
Zn2+

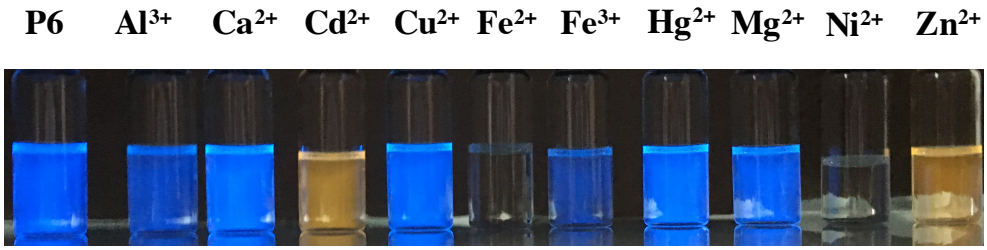
P6
Al3+
Ca2+
Cd2+
Cu2+
Fe2+
Fe3+
Hg2+
Mg2+
Ni2+
Zn2+

Fig. 4.

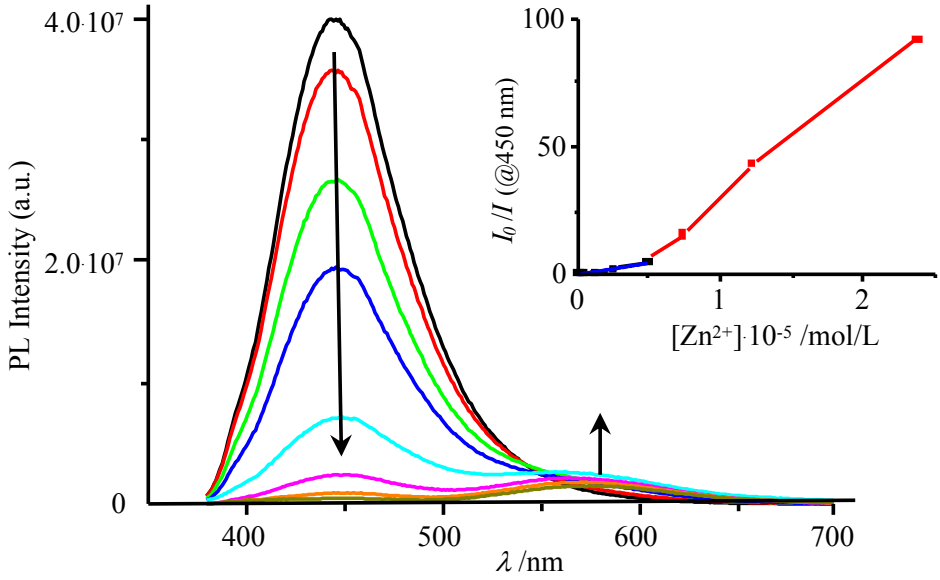
4.0·10⁷
2.0·10⁷
0
PL Intensity (a.u.)
400
500
600
700
λ /nm
100
50
0
0
1
2
I0 /I (@450 nm)
[Zn2+]·10-5 /mol/L

Fig. 5

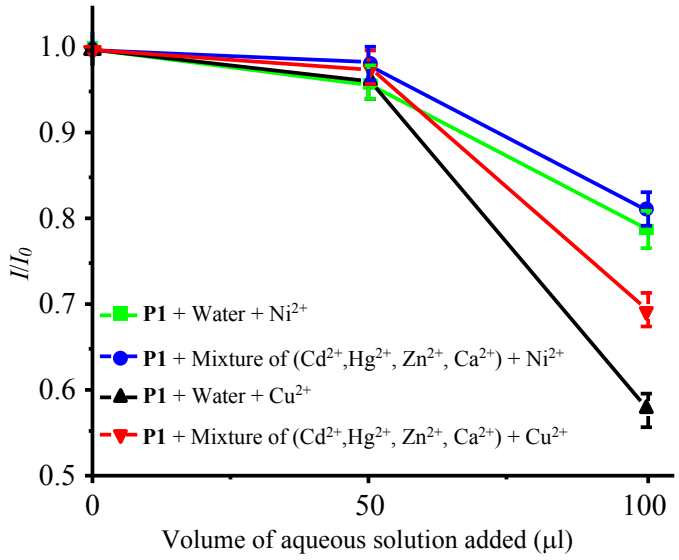
1.0
0.9
0.8
0.7
0.6
0.5
I/I_0
0
50
100
Volume of aqueous solution added (μl)
P1 + Water + Ni^{2+}
P1 + Mixture of (Cd^{2+},Hg^{2+}, Zn^{2+}, Ca^{2+}) + Ni^{2+}
P1 + Water + Cu^{2+}
P1 + Mixture of (Cd^{2+},Hg^{2+}, Zn^{2+}, Ca^{2+}) + Cu^{2+}

Fig. 6

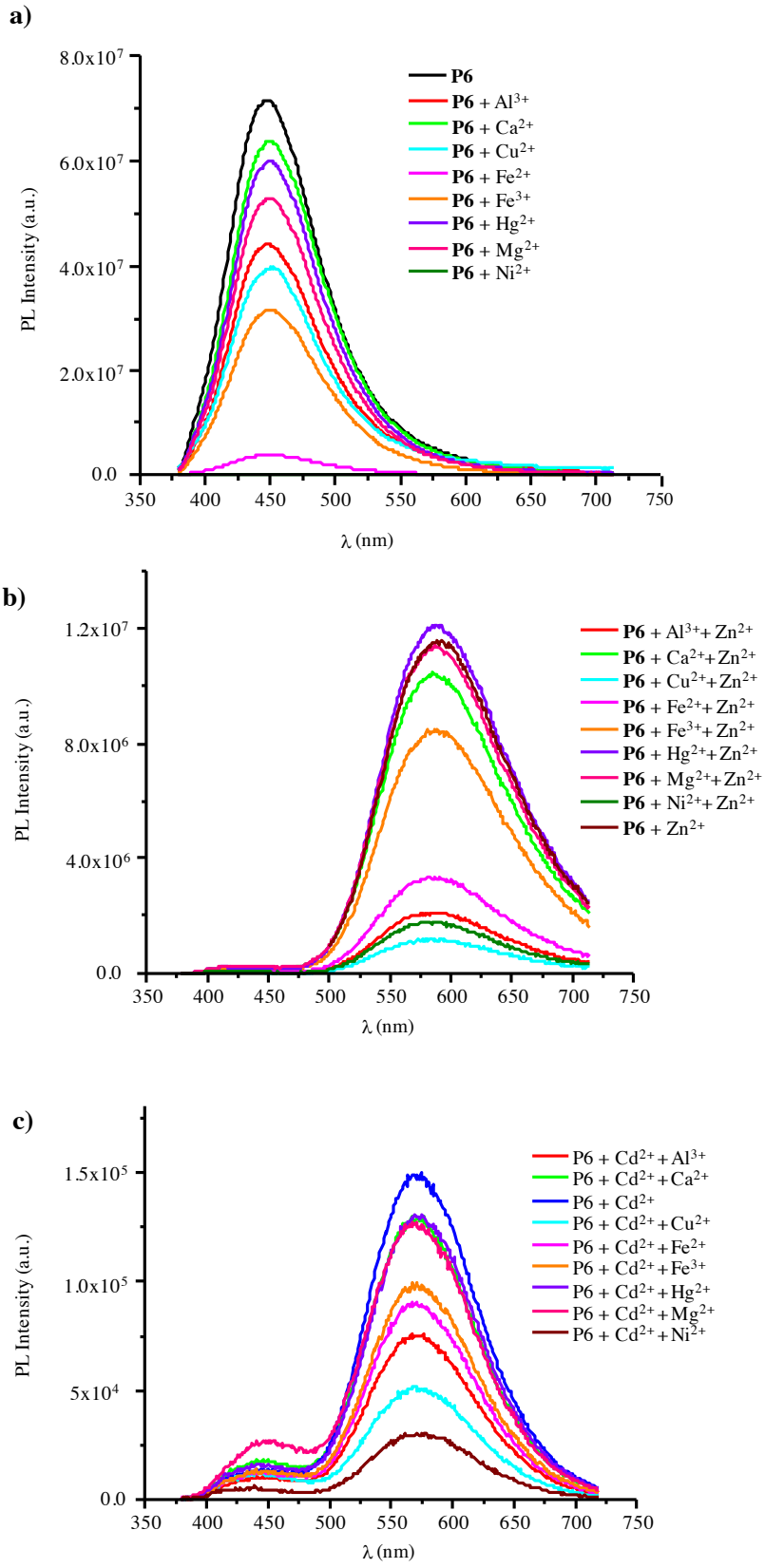
a)
8.0x10^7
6.0x10^7
4.0x10^7
2.0x10^7
0.0
PL Intensity (a.u.)
350 400 450 500 550 600 650 700 750
λ (nm)
P6
P6 + Al3+
P6 + Ca2+
P6 + Cu2+
P6 + Fe2+
P6 + Fe3+
P6 + Hg2+
P6 + Mg2+
P6 + Ni2+
b)
1.2x10^7
8.0x10^6
4.0x10^6
0.0
PL Intensity (a.u.)
350 400 450 500 550 600 650 700 750
λ (nm)
P6 + Al3+ + Zn2+
P6 + Ca2+ + Zn2+
P6 + Cu2+ + Zn2+
P6 + Fe2+ + Zn2+
P6 + Fe3+ + Zn2+
P6 + Hg2+ + Zn2+
P6 + Mg2+ + Zn2+
P6 + Ni2+ + Zn2+
P6 + Zn2+
c)
1.5x10^5
1.0x10^5
5x10^4
0.0
PL Intensity (a.u.)
350 400 450 500 550 600 650 700 750
λ (nm)
P6 + Cd2+ + Al3+
P6 + Cd2+ + Ca2+
P6 + Cd2+
P6 + Cd2+ + Cu2+
P6 + Cd2+ + Fe2+
P6 + Cd2+ + Fe3+
P6 + Cd2+ + Hg2+
P6 + Cd2+ + Mg2+
P6 + Cd2+ + Ni2+

Fig. 7

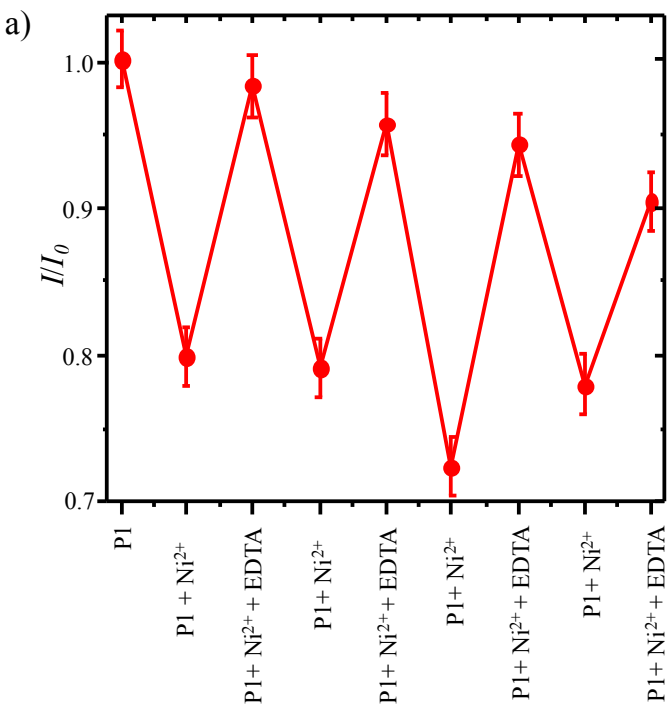
a)
1.0
0.9
0.8
0.7
I/I_0
P1
P1 + Ni^{2+}
P1+ Ni^{2+} + EDTA
P1+ Ni^{2+}
P1+ Ni^{2+} + EDTA
P1+ Ni^{2+}
P1+ Ni^{2+} + EDTA
P1+ Ni^{2+}
P1+ Ni^{2+} + EDTA

Fig. 8

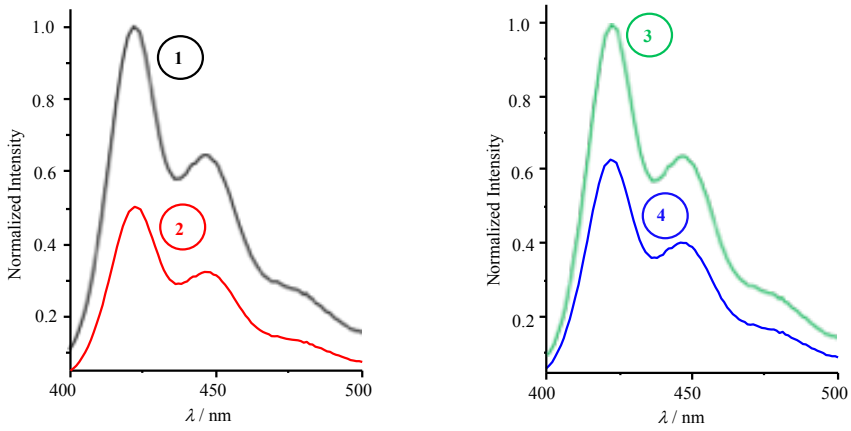
1.0
0.8
0.6
0.4
0.2
Normalized Intensity
1
2
400
450
500
λ / nm
1.0
0.8
0.6
0.4
0.2
Normalized Intensity
3
4
400
450
500
λ / nm

Fig. 9

Optical chemosensors for metal ions in aqueous medium with polyfluorene derivatives: sensitivity, selectivity and regeneration

Xinyang Wang,[a] Qiqiao Lin,[a] Sasikumar Ramachandran,[a] Gaëlle Pembouong,[b] Robert B. Pansu,[c] Isabelle Leray,[c] Bérengère Lebental, [a,d] Gaël Zucchi*[a]

Table legends

Table 1. Photophysical data for **M1**-**M3** and **P1**-**P6** in THF solutions.

Table 2. Summary of the selectivity of **M1**, **M2**, and **M3** towards metal ions as indicated by fluorescence studies.

Table 3. Summary of the selectivity of **P1**–**P6** towards metal ions.

Table 4. Values of the Stern-Volmer constants (M^{-1}) for **P1**, **P3**, **P4**, and **P6**.

Table 5. Limits of detection (in ppb) for **P1**, **P3**, **P4**, and **P6** for several metal ions.

Table 1. Photophysical data for **M1**-**M3** and **P1**-**P6** in THF solutions.

Compound	λ_{abs}^{max}/nm	$\lambda_{em}^{max}(\lambda_{exc})$ /nm	Q (±10%)
M1[a]	304	373 (305)	9
M2[a]	303	346 (305)	12
M3[a]	302	410 (330)	14
P1[b]	377	421 (380)	39
P2[b]	375	420 (380)	61
P3[b]	382	421 (390)	67
P4[b]	314	402 (370)	36
P5[b]	346	404 (350)	57
P6[b]	353	450 (360)	39

[a] Concentrations of the three monomers were 2×10^{-5} M and 4×10^{-5} M for recording the absorption and emission spectra, respectively.

[b] Absorption and emission of the polymers were measured with solutions having concentration of 0.1 mg/ml and 5 μg/ml, respectively.

Table 2. Summary of the selectivity of **M1**, **M2**, and **M3** towards metal ions as indicated by fluorescence studies.

Monomer	Selectivity to ion
M1	Ni^{2+}, Cu^{2+}, Ca^{2+}
M2	Fe^{3+}, Al^{3+}
M3	Ni^{2+}, Cu^{2+}, Zn^{2+}, Cd^{2+}, Fe^{2+}

Table 3. Summary of the selectivity of **P1**–**P6** towards metal ions.

Polymer	Ligand	Ligand content (%)	Selectivity to ion
P1	**M1**	11	Ni^{2+}, Cu^{2+}
P2	**M2**	11	-
P3	**M3**	3	Ni^{2+}, Cu^{2+}, Zn^{2+}, Ca^{2+}, Al^{3+}
P4	**M1**	50	Ni^{2+}, Cu^{2+}, Ca^{2+}, Al^{3+}
P5	**M2**	44	-
P6	**M3**	50	Ni^{2+}, Cu^{2+}, Zn^{2+}, Ca^{2+}, Al^{3+}, Cd^{2+}, Fe^{2+}

Table 4. Values of the Stern-Volmer constants (M^{-1}) for **P1**, **P3**, **P4**, and **P6**.

Polymer	Ni^{2+}	Cu^{2+}	Zn^{2+}	Ca^{2+}	Al^{3+}	Fe^{2+}	Cd^{2+}
P1	$2.1 \cdot 10^6$	$3.0 \cdot 10^5$					
P3	$5.9 \cdot 10^6$	$9.0 \cdot 10^5$	$9.9 \cdot 10^5$	$2.6 \cdot 10^5$	$6.1 \cdot 10^5$		
P4	$2.0 \cdot 10^6$	$5.4 \cdot 10^5$		$2.8 \cdot 10^5$	$6.7 \cdot 10^4$		
P6	$2.0 \cdot 10^6$	$8.0 \cdot 10^5$	$9.3 \cdot 10^5$	$3.1 \cdot 10^5$	$2.0 \cdot 10^5$	$1.3 \cdot 10^5$	$6.0 \cdot 10^5$

Table 5. Limits of detection (in ppb) for **P1**, **P3**, **P4**, and **P6** for several metal ions.

Polymer	Ni^{2+}	Cu^{2+}	Zn^{2+}	Ca^{2+}	Al^{3+}	Fe^{2+}	Cd^{2+}
P1	1.7	12.7					
P3	0.6	4.2	4.0	9.2	2.7		
P4	1.8	14.1		8.6	24.2		
P6	1.8	4.8	4.2	7.8	8.1	17.6	11.2